

# Low Phase Noise, High Output Power and Compact Microwave Planar Oscillator for C-Band Applications

Hanae El Ftouh<sup>1,\*</sup>, Moustapha El Bakkali<sup>1</sup>, Aicha Mchbal<sup>1</sup>,  
Soukaina Sekkal<sup>2</sup>, and Naima Amar Touhami<sup>1</sup>

<sup>1</sup>Laboratory of Intelligent and Systems Design, Team of Electronic and Smart Systems  
Department of Physics, Faculty of Sciences, Tetouan, Morocco

<sup>2</sup>Laboratory Optic, Systems and Materials, Department of Physics, Faculty of Sciences, Tetouan, Morocco

**ABSTRACT:** In this paper, a novel microwave oscillator is developed at frequencies of 5.7 and 7.5 GHz through the application of Negative Resistance and Harmonic Balance theory. The design process involves leveraging the Agilent Advance Design System (ADS) tool, ensuring exceptional electromagnetic (EM) performance. The utilization of microstrip circuit elements enhances the overall performance of the oscillator structure. Following optimization and co-simulation of nonlinear models for the compact Planar Microwave Oscillator ( $62 \times 38 \text{ mm}^2$ ), highly satisfactory results are obtained. Quantitatively, the measured output powers at 5.7 and 7.5 GHz are determined to be 9.5 dBm and 7.05 dBm, respectively. These power levels are particularly relevant for C band applications spanning 4 to 8 GHz, including areas such as satellite communication, radar, and wireless networks.

## 1. INTRODUCTION

An oscillator is an autonomous circuit capable of sustaining a steady-state oscillation at a frequency different from those delivered by input generators or their harmonic frequencies. The most obvious example is free-running oscillator, which generates a periodic solution from the energy delivered by direct-current (DC) sources only. There is no external excitation [1–4].

Oscillators are commonly found in computers, wireless receivers and transmitters, audio-frequency equipment, and music synthesizers. They serve as the signal source for all microwave systems, encompassing both transmitters and receivers. These components are integral to various electronic systems, such as Global System for Mobile Communication (GSM), radio communication, spatial communication, radar, electronic warfare, and instrumentation, due to their ability to create electrical signals in different frequency ranges. Moreover, the quality of any system directly depends on the performance of the oscillator [5]. Consequently, the study of stability and phase noise analysis constitutes a comprehensive set of tools for efficiently and accurately predicting autonomous circuit behavior [1, 6, 7]. The harmonic balance method is a technique employed for the numerical solution of nonlinear analog circuits operating in a periodic, quasi-periodic, and steady-state regime. This method proves useful in deriving the continuous wave response of numerous nonlinear microwave components, including amplifiers, mixers, and oscillators [8–12].

A microwave oscillator typically comprises four separate blocks: a resonator for selecting the oscillation frequency, a

transistor (an active device) operating at the desired frequency, and polarization and instability blocks. The block diagram of the microwave oscillator, illustrating its various components, is presented in Figure 1 [13].

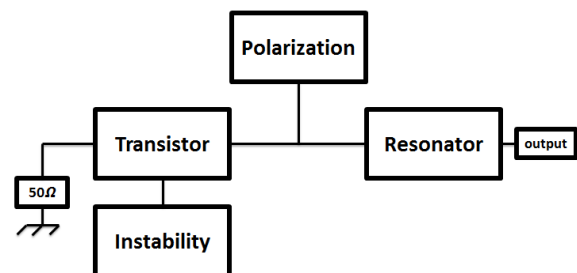


FIGURE 1. Different blocks constituting an oscillator.

In the subsequent sections, we will delve into the study of a new dual-band negative resistance oscillator design aimed at reducing phase noise, enhancing frequency stability, achieving high efficiency, and generating significant output power.

To accomplish this, we will analyze each block constituting it in depth to optimize the various performances of the entire circuit. Initially, we will begin by scrutinizing the bias network of the oscillator. The subsequent step involves studying the resonator, which is based on two band-pass filters resonating respectively at 5.7 and 7.5 GHz, while also detailing the instability aspects of the circuit. Our approach commences with electric simulation to determine the initial values of the studied circuit, followed by electromagnetic simulation for the PCB circuit to account for coupling effect. The final step involves co-simulation to integrate both passive and active components.

\* Corresponding author: Hanae El Ftouh (elftouhhanac2@gmail.com).

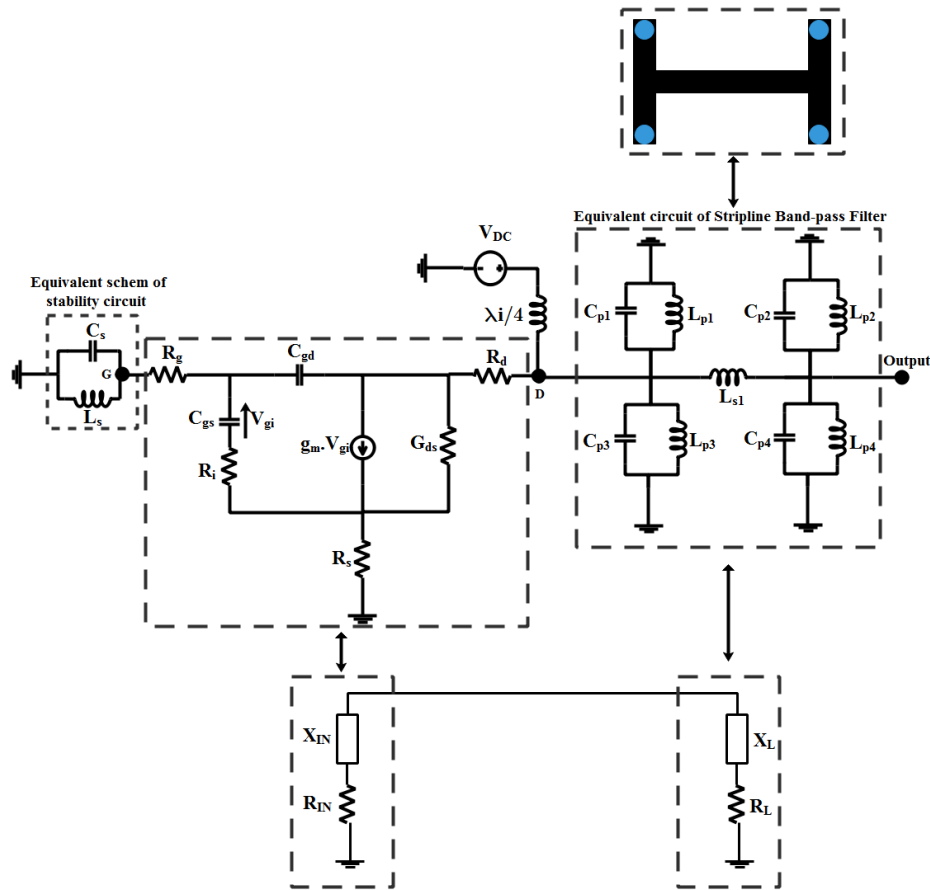


FIGURE 2. Equivalent circuit of the proposed negative resistance oscillator.

The active device employed is an MG4918D HEMT transistor, whose model is available in the advanced design system (ADS) simulator. This transistor is applicable to a frequency range from 1 to 18 GHz. Furthermore, the substrate utilized is FR4, with the following characteristics: a length ( $h$ ) of 1.6 mm, a thickness ( $T$ ) of 35  $\mu\text{m}$ , a loss tangent ( $\tan \delta$ ) of 0.02, and a relative permittivity ( $\epsilon_r$ ) of 4.6.

## 2. LINEAR ANALYSIS OF OSCILLATOR

Several methods can be employed to determine the fundamental conditions for oscillation. In this section, we will elaborate on the negative resistance method.

The input impedance of a system with negative resistance is contingent upon both the amplitude and frequency of the signal [14].

$$Z_{in}(A, j\omega) = R_{IN} + jX_{IN}$$

where  $A$  is the amplitude of current  $i(t)$ .

$$Z_{in}(A, j\omega) < 0$$

For oscillations to start, a condition must be satisfied:

$$R_{IN} + R_L < 0$$

Oscillations are the result of random noise (usually thermal noise in resistors). This noise enters a cumulative process and amplifies. Each time the current amplitude increases, the resistance becomes less negative and, at some point, converges

towards zero. Then, at a nominal current value, a steady state is established.

The equations describing the steady state areas are follows:

$$R_{IN} + R_L = 0 \quad \text{and} \quad X_{IN} = X_L^*$$

For a general nonlinear active device, determining the conditions for maximizing the power delivered to a load can be addressed in a quasi-linear approximation. This can be achieved by employing the large-signal impedance or admittance two-port parameters, which are functions of a single port voltage [15].

The equivalent circuit of the studied oscillator is shown in Figure 2.

## 3. OSCILLATOR DESIGN PROCESS

### 3.1. Bias Network

The bias network comprises three ports [16]. The low-frequency port is utilized to inject the polarization (DC signal at  $P_3$ ); the high-frequency port is employed for injecting the radiofrequency signal (RF signal at  $P_1$ ); and the third port serves as an output where the radiofrequency plus direct current (DC) signal is recovered at  $P_2$ . Figure 3 illustrates the bias network at both frequencies, 5.7 and 7.5 GHz.

The EM simulation results of  $S$  parameters at both frequencies are shown in Figure 4. We can observe that at 5.7 and

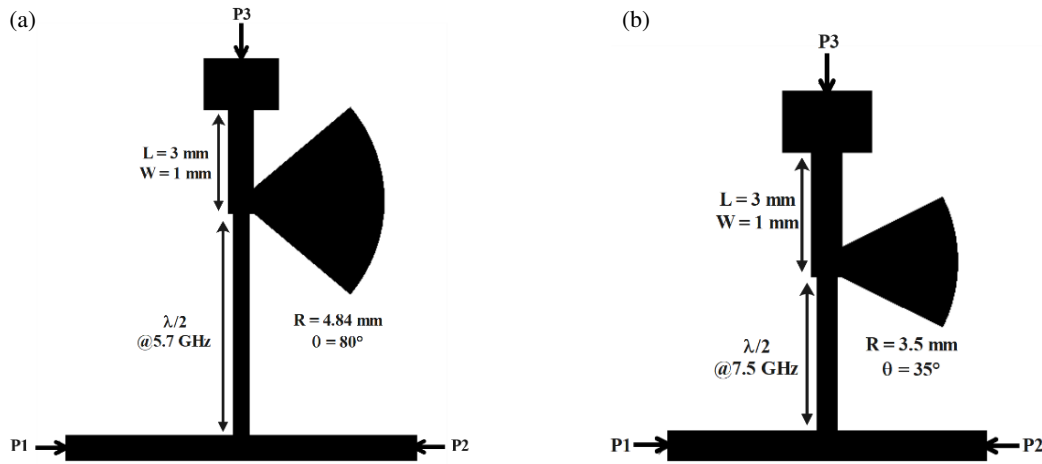


**FIGURE 3.** Proposed layout for bias circuits for applications: (a) Satellite communication and radar, and (b) wireless networks.

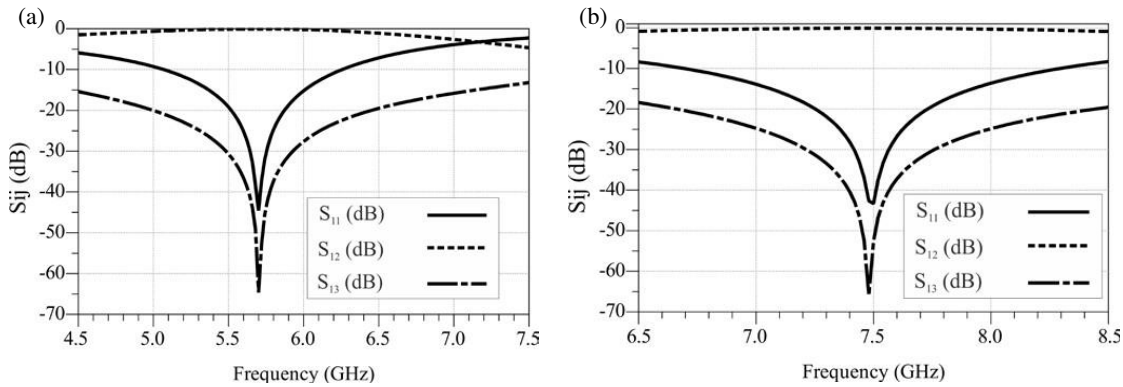


**FIGURE 4.** Result of EM simulation of bias circuits centered at 5.8 GHz and 7.5 GHz.

7.5 GHz, the inverse gain  $S_{12}$  is equal to 0 dB, meaning that the signal is transmitted completely. Regarding the  $S_{11}$  parameter, we observe that the adaptation in both cases is below  $-40$  dB, and the isolation  $S_{13}$  is approximately  $-65$  dB, indicating satisfactory isolation between the radio frequency (RF) and DC sources.

### 3.2. Study of Stability

The  $S$ -parameter formulation was introduced by Rollet factor  $K$ , which states that for absolute instability [17], two conditions must apply:

$$K < 1 \quad \text{and} \quad B < 0$$

$K$  and  $B$  are respectively the stability factor and measurement stability:

$$K = \frac{1 - |S_{11}|^2 - |S_{22}|^2 + |S_{11}S_{22} - S_{12}S_{21}|}{2|S_{12}S_{21}|}$$

$$B = 1 + |S_{11}|^2 + |S_{22}|^2 + |\Delta|^2$$

where

$$\Delta = S_{22} \cdot S_{11} - S_{12} \cdot S_{21}$$

In practice,  $K < 1$  is widely accepted by the microwave community as the condition for absolute stability [17, 18]. The Rollet or stability factor  $K$  is employed only for simple two-port

circuit. As our circuit features 4 ports, the expression for  $K$  is not applicable. Instead, the reflection coefficients  $S_{ii}$  of the circuit are utilized to satisfy the Barkhausen condition, the prerequisites for initiating oscillations. In this scenario, it is necessary to have  $S_{ii} > 0$  dB. Figure 5 illustrates the conditions for initiating oscillations at both frequencies (5.7 and 7.5 GHz), demonstrating that the oscillation criterion is met at both frequencies. Specifically, at these frequencies, the parameters  $S_{11}$ ,  $S_{22}$ ,  $S_{33}$ , and  $S_{44}$  are all greater than 0.

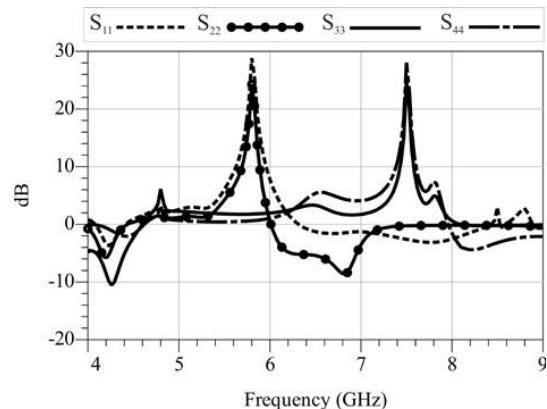


**FIGURE 5.** Instability co-simulation result of the proposed oscillator.

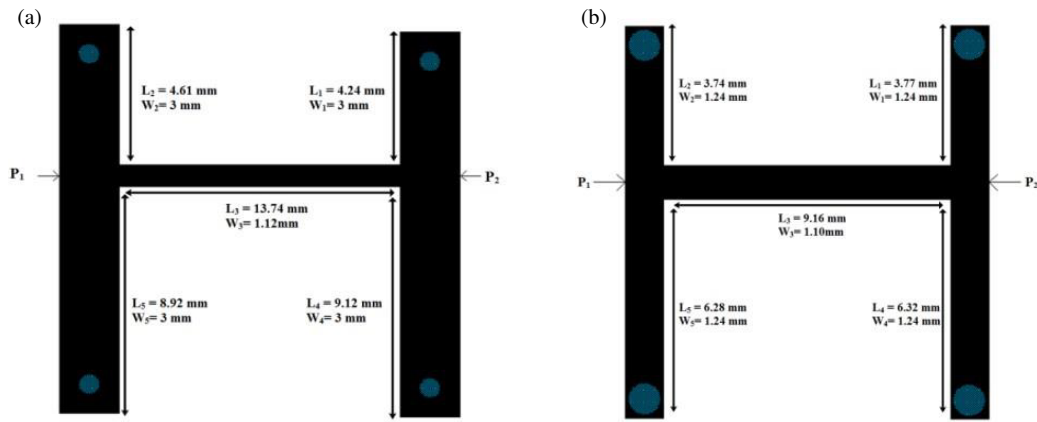


**FIGURE 6.** Layout of the band pass filters proposed for C-band applications: (a) WLAN Communication; (b) Satellite Communication.

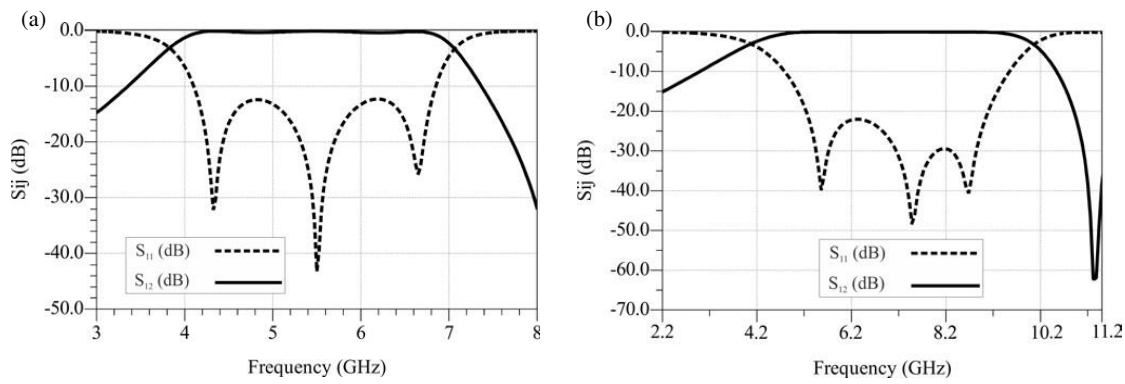


**FIGURE 7.** Response of bandpass filters operating at: (a) WLAN communication; (b) Satellite communication.

### 3.3. Resonator

The resonator of our oscillator comprises two bandpass filters, as depicted in Figure 6. One resonates at 5.7 GHz, designed for WLAN communication and radio telecommunication, while the other filter resonates at 7.5 GHz, intended for satellite communication and radar. Both frequencies belong to the C band. The primary function of these two resonators is to suppress the harmonic spectrum.

Figure 7 displays the simulation results of the  $S_{11}$  and  $S_{12}$  parameters for the proposed resonators. It is evident from the EM simulation that the  $S_{11}$  parameter is less than  $-30$  dB, and the  $S_{12}$  parameter tends toward 0 dB, indicating excellent adaptation and transmission in both cases. The circuits are primarily designed to achieve the desired frequencies for the load.

## 4. RESULTS OF STUDIED NEGATIVE RESISTANCE OSCILLATOR

In this section, we will examine the performance of the studied oscillator in terms of output power and the level of phase noise determined through co-simulation. It is important to note that these noise sources are distributed in the active component and have different origins depending on the type of transistors used (MOSFET, MESFET, HBT, etc.) [19]. First, in Figure 8, we

present the final layout of the proposed oscillator, including all its component parts with resistor values  $R_1$  and  $R_2$  set to  $50 \Omega$ .

In Figure 9, we illustrate the typical output spectrum of the oscillator at both frequencies. The oscillation frequencies are 5.7 GHz and 7.5 GHz, which are employed for WLAN Radar and Satellite Communication applications. The oscillator yields a simulated output power of 11.095 dBm at 5.7 GHz and 8.259 dBm at 7.5 GHz.

The final circuit was manufactured by etching a metal layer on the substrate and soldering an Agilent MGF4918D InGaAs HEMT transistor along with lumped elements, as depicted in Figure 10.

The output spectrum of our fabricated oscillator, measured using a Rohde & Schwarz FSL spectrum analyzer, is depicted in Figure 11. The oscillator demonstrates stable oscillations at both frequencies of 5.7 GHz and 7.5 GHz, consistent with the expected results from the simulation. The output power of the fundamental oscillating signals at 5.6 and 7.5 GHz is measured, respectively, at the bias condition of  $V_{DS1} = V_{DS2} = 3.9$  V as 9.5 dBm and 7.05 dBm, considering cable losses of 6 dBm (the cable length is 150 cm).

Figure 12 illustrates the phase noise levels of the examined oscillator at  $P_1$  and  $P_2$  for frequencies of 100 kHz, 1 MHz, and 10 MHz. Table 1 provides a summary of the results depicted in the aforementioned figure.

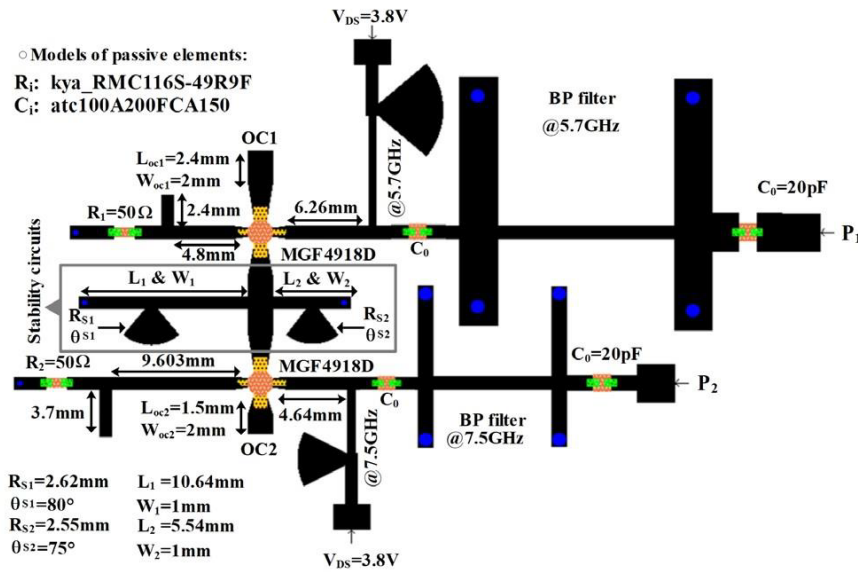


FIGURE 8. Completed layout of the proposed dual-output oscillator.

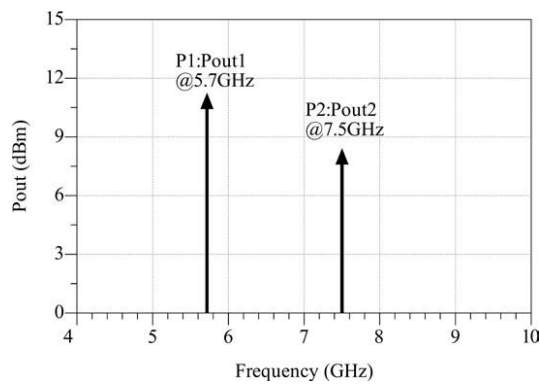
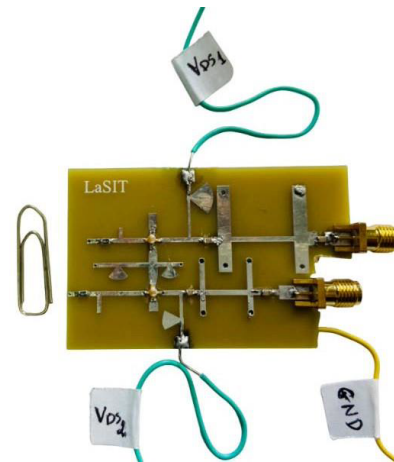
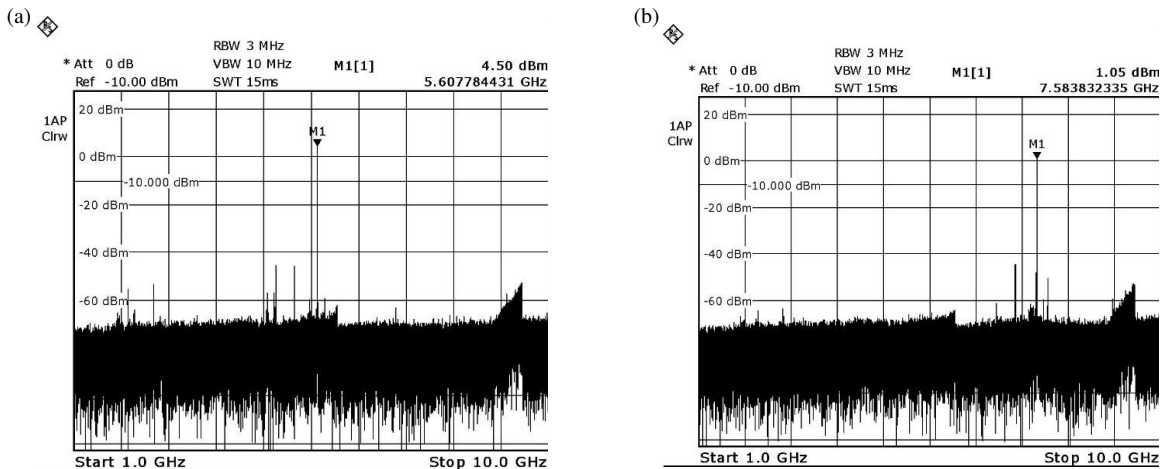
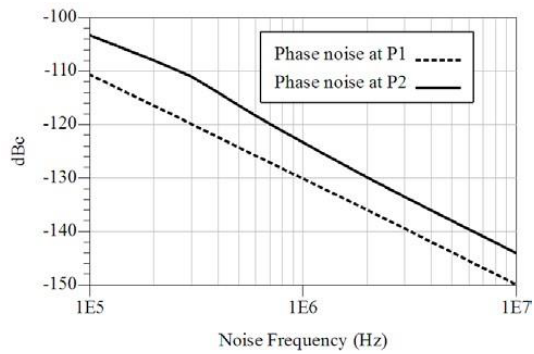


FIGURE 9. Co-simulation result of the output power spectrum at 5.7 GHz and 7.5 GHz.

FIGURE 10. Image of the realized prototype of the dual-output oscillator ( $62 \times 38 \text{ mm}^2$ ).FIGURE 11. Measurement result of the dual-output oscillator for  $V_{DSi} = 3.9 \text{ V}$ .





**FIGURE 12.** Level of phase noise at 100 kHz, 1 MHz and 10 MHz.

As shown in Table 1, we can summarize that the phase noise was measured, and its values are  $-110.07$  dBc/Hz,  $-130.1$  dBc/Hz, and  $-150$  dBc/Hz at the offsets of 100 kHz, 1 MHz, and 10 MHz, respectively, at Port 1. Simultaneously, at Port 2, the phase noise was measured, and its values are  $-103.3$  dBc/Hz,  $-123.3$  dBc/Hz, and  $-144$  dBc/Hz at the offsets of 100 kHz, 1 MHz, and 10 MHz, respectively.

**TABLE 1.** Summary of noise phase values.

Phase Noise (dBc/Hz)	@100 kHz	@1 MHz	@10 MHz
At P1	$-110.7$	$-130.1$	$-150$
At P2	$-103.3$	$-123.3$	$-144$

## 5. CONCLUSION

A dual-output negative resistance oscillator designed for WLAN, Radar, and Satellite Communication applications is developed in this paper. The EM studied circuit exhibits oscillations and provides simulated output power of  $11.095$  dBm at  $5.7$  GHz and  $8.259$  dBm at  $7.5$  GHz. The measured output power of the oscillator, operating at  $5.6$  and  $7.5$  GHz, was recorded as  $9.5$  dBm and  $7.05$  dBm, respectively. Additionally, the oscillator demonstrates significantly low phase noise at both ports, measuring  $-110.07$  dBc/Hz,  $-130.1$  dBc/Hz, and  $-150$  dBc/Hz at the offsets of 100 kHz, 1 MHz, and 10 MHz, respectively, at Port 1. Meanwhile, at Port 2, the phase noise was measured as  $-103.3$  dBc/Hz,  $-123.3$  dBc/Hz, and  $-144$  dBc/Hz at the offsets of 100 kHz, 1 MHz, and 10 MHz, respectively.

## REFERENCES

- [1] Rohde, U. L., A. K. Poddar, and G. Böck, *The Design of Modern Microwave Oscillators for Wireless Applications: Theory and Optimization*, John Wiley & Sons, Jun. 2005.
- [2] Rhea, R. W., "A new class of oscillators," *IEEE Microwave Magazine*, Vol. 5, No. 2, 72–83, Jun. 2004.
- [3] Van Delden, M., N. Pohl, K. Aufinger, C. Baer, and T. Musch, "A low-noise transmission-type Yttrium Iron Garnet tuned oscillator based on a SiGe MMIC and bond-coupling operating up to 48 GHz," *IEEE Transactions on Microwave Theory and Techniques*, Vol. 67, No. 10, 3973–3982, Oct. 2019.
- [4] Li, B., Y. Liu, C. Yu, and Y. Wu, "A novel concurrent dual-band oscillator based on a single ring resonator," *IEEE Microwave and Wireless Components Letters*, Vol. 26, No. 8, 607–609, Aug. 2016.
- [5] Malki, A., J. Zbitou, L. E. Abdellaoui, M. Latrach, A. Tajmouati, and A. Errkik, "Design of negative resistance oscillator with record low phase noise," *Telecommunication Computing Electronics and Control*, Vol. 16, No. 2, 586–593, Apr. 2018.
- [6] Ramesh, S., M. Nithin, and H. M. Kittur, "Design of millimeter wave LC oscillators for 5G applications," in *2019 International Conference on Communication and Signal Processing (ICCSP)*, 4–6, India, Apr. 2019.
- [7] Hu, Y., T. Siriburanon, and R. B. Staszewski, "A 30-GHz class-F23 oscillator in 28 nm CMOS using harmonic extraction and achieving 120 kHz 1/f3 corner," in *43rd IEEE European Solid State Circuits Conference*, 87–90, Leuven, Belgium, Sep. 2017.
- [8] Gilmore, R. J. and M. B. Steer, "Nonlinear circuit analysis using the method of harmonic balance - A review of the art. Part I. Introductory concepts," *International Journal of Microwave and Millimeter-wave Computer-Aided Engineering*, Vol. 1, No. 1, 22–37, Jan. 1991.
- [9] Hajder, T., "Higher order loops improve phase noise of feedback oscillators," *Applied Microwave and Wireless*, Vol. 14, No. 10, 24–31, 2002.
- [10] Rizzoli, V., A. Costanzo, D. Masotti, A. Lipparini, and F. Matri, "Computer-aided optimization of nonlinear microwave circuits with the aid of electromagnetic simulation," *IEEE Transactions on Microwave Theory and Techniques*, Vol. 52, No. 1, 362–377, Jan. 2004.
- [11] Cheng, K. M. and K. P. Chan, "Power optimization of high-efficiency microwave MESFET oscillators," *IEEE Transactions on Microwave Theory and Techniques*, Vol. 48, No. 5, 787–790, May 2000.
- [12] Dyskin, A., S. Wagner, and I. Kallfass, "A compact resistive quadrature low noise Ka-band VCO SiGe HBT MMIC," in *2019 12th German Microwave Conference (GeMiC)*, 95–98, Stuttgart, Germany, Mar. 2019.
- [13] Benakaprasad, B., S. Sharabi, and K. Elgaid, "RF and microwave oscillator design using p-HEMT transistor," *International Journal of Scientific and Research Publications*, Vol. 4, No. 8, 1–7, 2014.
- [14] Jovanović, P., S. Tasić, and B. Jokanović, "Voltage-controlled oscillator at 6 GHz for doppler radar in heart sensing applications," *Serbian Journal of Electrical Engineering*, Vol. 6, No. 3, 471–478, Dec. 2009.
- [15] Grebennikov, A., *RF and Microwave Transistor Oscillator Design*, John Wiley & Sons, 2007.
- [16] El Bakkali, M., N. A. Touhami, H. E. Ftouh, and A. Marroun, "Design of 5.2 GHz low noise amplifier for wireless LAN," in *Procedia Manufacturing*, Vol. 32, 739–744, Tirgu Mures, Romania, Oct. 2019.
- [17] Rollett, J., "Stability and power-gain invariants of linear twoports," *IRE Transactions on Circuit Theory*, Vol. 9, No. 1, 29–32, 1962.
- [18] Platzker, A. and W. Struble, "Rigorous determination of the stability of linear N-node circuits from network determinants and the appropriate role of the stability factor K of their reduced twoports," in *Third International Workshop on Integrated Nonlinear Microwave and Millimeterwave Circuits*, 93–107, Duisburg, Germany, 1994.
- [19] Prigent, M., M. Camiade, J. C. Nallatamby, J. Guittard, and J. Obregon, "An efficient design method of microwave oscillator circuits for minimum phase noise," *IEEE Transactions on Microwave Theory and Techniques*, Vol. 47, No. 7, 1122–1125, Jul. 1999.